Electronic Supplementary Material

Boron and nitrogen co-doped porous carbon derived from sodium alginate enhanced capacitive deionization for water purification

Xiao Yong[1], Pengfei Sha[1], Jinghui Peng[1], Mengdi Liu[1], Qian Zhang[1], Jianhua Yu (✉)[1], Liyan Yu (✉)[1], Lifeng Dong (✉)[1,2]

1 College of Materials Science and Engineering, Qingdao University of Science and Technology, Qingdao 266042, China

2 Department of Physics, Hamline University, St. Paul 55104, USA

E-mails: jianhuayu@qust.edu.cn (Yu J.); liyanyu@qust.edu.cn (Yu L.); donglifeng@qust.edu.cn (Dong L.)

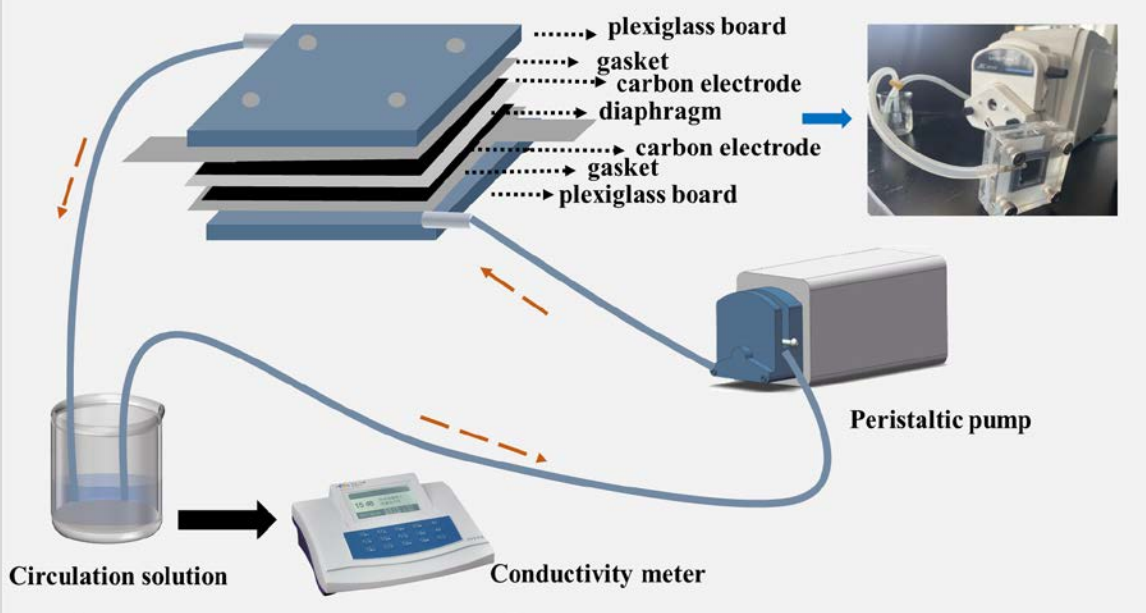

Fig. S1 Schematic illustration of the CDI system.

The etching reactions during KOH activation can be expressed as below [1].

$$6KOH + 2C \rightarrow 2K + 3H_2 + 2K_2CO_3 \quad (S1)$$

$$K_2CO_3 \rightarrow K_2O + CO_2 \quad (S2)$$

$$K_2CO_3 + 2C \rightarrow 2K + 3CO \quad (S3)$$

$$K_2O + C \rightarrow 2K + CO \quad (S4)$$

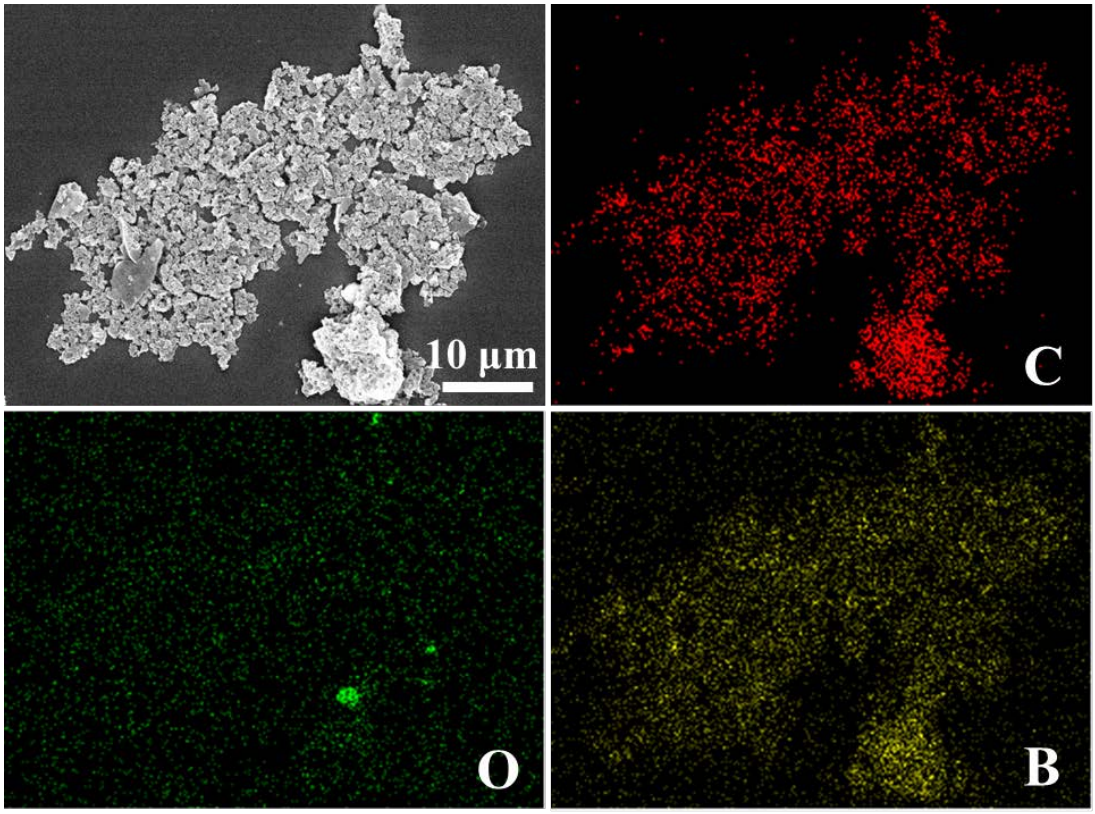

Fig. S2 SEM image of SAB and its corresponding C, O, B elemental mapping images.

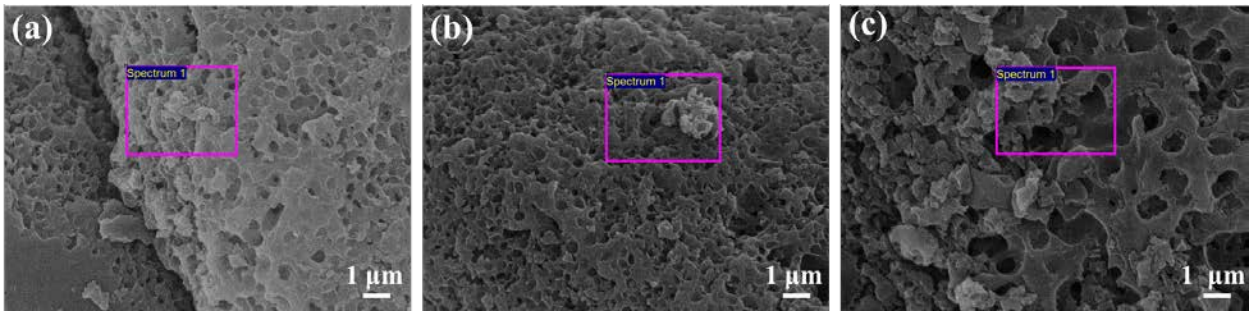

Fig. S3 SEM images of SA, SAB & SABN and the regions marked in pink for EDS analyses.

Table S1 Element contents of SA, SAB and SABN

	C	O	B	N
SA (at. %)	93.4	6.6	0	0
SAB (at. %)	85.6	6.9	8.5	0
SABN (at. %)	65.1	3.2	9.6	22.1

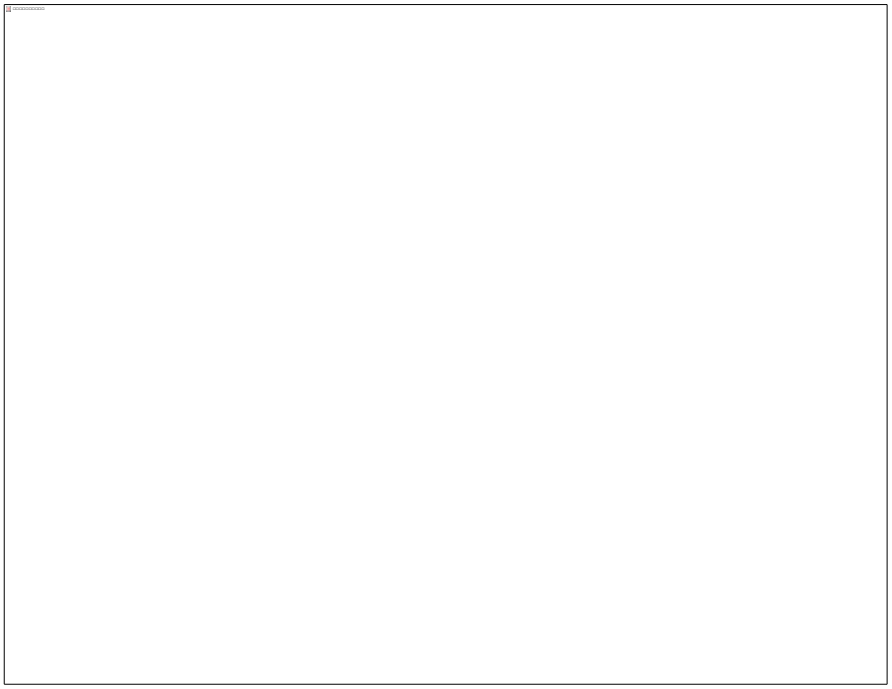

Fig. S4 BJH pore size distributions of three samples.

Table S2 Pore texture parameters of SA, SAB and SABN derived from N_2 adsorption data

	$S_{BET}/(m^2 \cdot g^{-1})^{a)}$	$S_{mic}/(m^2 \cdot g^{-1})^{b)}$	$S_{mes}/(m^2 \cdot g^{-1})^{c)}$	S_{mes}/S_{BET}	$V_t/(m^3 \cdot g^{-1})^{d)}$	$V_{mic}/(m^3 \cdot g^{-1})^{e)}$	V_{mic}/V_t
SA	3603.0	1155.4	2447.6	0.68	2.06	0.42	0.20
SAB	2739.1	621.6	2117.5	0.77	1.57	0.24	0.15
SABN	2587.1	727.6	1859.5	0.72	1.40	0.29	0.21

a) Specific surface area (S_{BET}) was calculated with modified Brunauer-Emmett-Teller (BET) method.

b) Micropore surface area (S_{mic}) was obtained from t-plot method.

c) Mesopore surface area (S_{mes}) was obtained from t-plot method.

d) Total pore volume (V_t) was estimated from the adsorbed amount at a relative pressure of 0.99.

e) Micropore volume (V_{mic}) was obtained from t-plot method.

Table S3 Impedance parameters of SA, SAB and SABN

	SA	SAB	SABN
R_s/Ω	3.05	2.70	2.75
R_{ct}/Ω	0.25	0.64	0.35

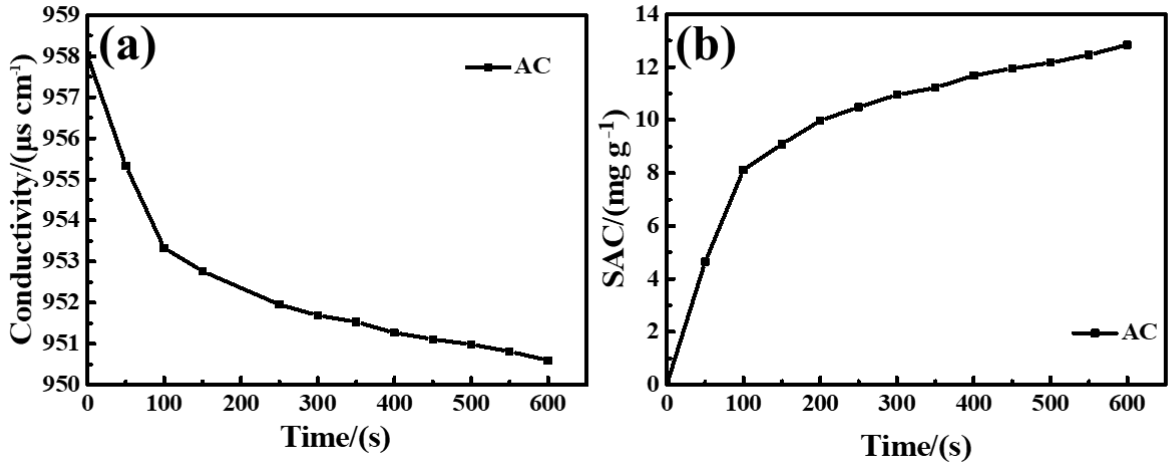

Fig. S5 (a) Electrosorption performance in NaCl solution with an initial concentration of 500 mg·L^{-1} at 1.2 V, and (b) variation of desalination capacity for commercial activated carbon.

Table S4 Comparison between SABN and other carbon electrodes.

Samples	Concentration/ (mg·L^{-1})	Working voltage/(V)	SAC/ (mg·g^{-1})	Reference
NPC-1.5	100	1.2	22.19	[2]
PCN6	1000	1.2	16.29	[3]
N-HPCA	500	1.2	17.9	[4]
P-CNFA0.02	1000	1.2	16.20	[5]
PPCP800	1000	1.2	14.62	[6]
SABN	500	1.2	26.9	This work

Figure S6. Cyclic regeneration curves of SABN in 500 mg L^{-1} NaCl solution.

The removal efficiency (%) was calculated by Eq. S5 [7].

$$\text{Removal efficiency} = \frac{(C_0 - C_t)}{C_0} \times 100\%$$

where C_0 indicates the initial ion concentration, and C_t represents the final concentration.

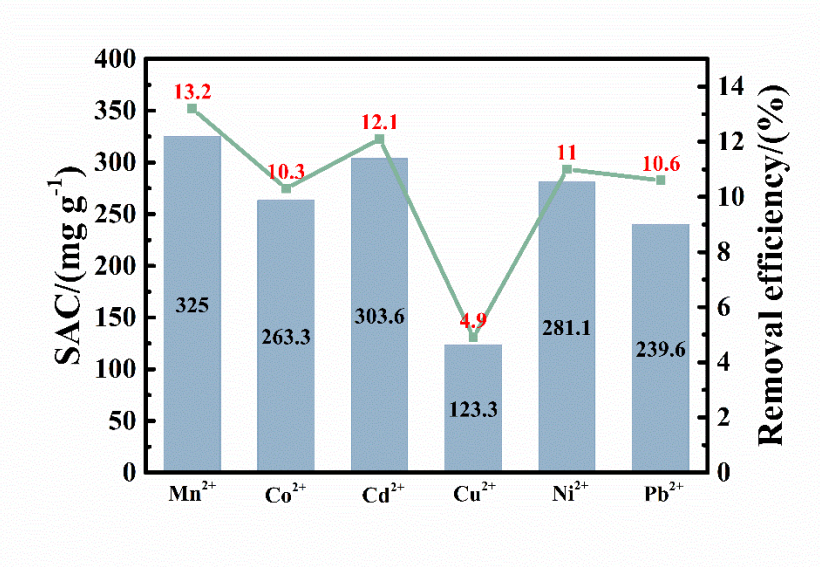

Fig. S7 Adsorption capacity and removal efficiency of different heavy metals on SABN electrode.

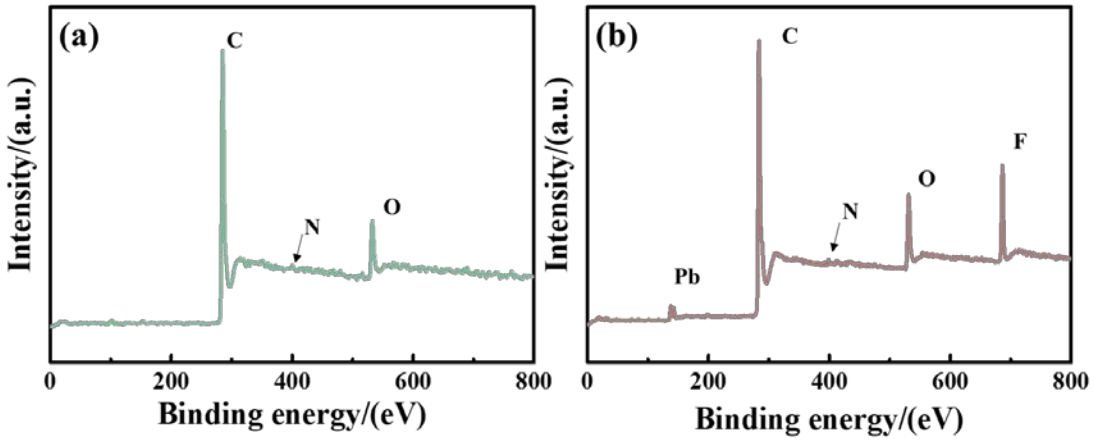

Fig. S8 XPS spectra of SABN electrode (a) before and (b) after Pb^{2+} adsorption.

References

1. Zhang D, Sun L, Liu Q, Sun H, Wang Q, Li W, Li Z, Wang B. Ultra-high specific surface area porous carbon derived from chestnut for high-performance supercapacitor. Biomass and Bioenergy, 2021, 153: 106227.

2. Zheng S-M, Yuan Z-H, Dionysiou D D, Zhong L-B, Zhao F, Yang J-C E, Zheng Y-M. Silkworm cocoon waste-derived nitrogen-doped hierarchical porous carbon as robust electrode materials for efficient capacitive desalination. Chemical Engineering Journal, 2023, 458: 141471

3. Lu T, Liu Y, Xu X, Pan L, Alothman A A, Shapter J, Wang Y, Yamauchi Y. Highly efficient water desalination by capacitive deionization on biomass-derived porous carbon nanoflakes. Separation and Purification Technology, 2021, 256: 117771.

4. Liu X, Liu H, Mi M, Kong W, Ge Y, Hu J. Nitrogen-doped hierarchical porous carbon aerogel for high-performance capacitive deionization. Separation and Purification Technology, 2019, 224: 44-50.

5. Li Y, Liu Y, Wang M, Xu X, Lu T, Sun C Q, Pan L. Phosphorus-doped 3D carbon nanofiber aerogels derived from bacterial-cellulose for highly-efficient capacitive deionization. Carbon, 2018, 130: 377-383.

6. Xing W, Zhang M, Liang J, Tang W, Li P, Luo Y, Tang N, Guo J. Facile synthesis of pinecone biomass-derived phosphorus-doping porous carbon electrodes for efficient electrochemical salt removal. Separation and Purification Technology, 2020, 251: 117357.

7. Sun Y, Su Y, Zhao Z, Zhao J, Ye M, Wen X. Capacitive heavy metal ion removal of 3D self-supported nitrogen-doped carbon-encapsulated titanium nitride nanorods via the synergy of faradic-reaction and electro-adsorption. Chemical Engineering Journal, 2022, 443: 136542.